IEEE TRANSACTIONS ON ROBOTICS

Design and Validation of a Cable-Driven Asymmetric Back Exosuit

Jared M. Li[®], Dean D. Molinaro[®], *Student Member, IEEE*, Andrew S. King[®], Anirban Mazumdar[®], *Member, IEEE*, and Aaron J. Young[®]

Abstract—Lumbar spine injuries caused by repetitive lifting rank as the most prevalent workplace injury in the United States. While these injuries are caused by both symmetric and asymmetric lifting, asymmetric is often more damaging. Many back devices do not address asymmetry, so we present a new system called the Asymmetric Back Exosuit (ABX). The ABX addresses this important gap through unique design geometry and active cable-driven actuation. The suit allows the user to move in a wide range of lumbar trajectories while the "X" pattern cable routing allows variable assistance application for these trajectories. We also conducted a biomechanical analysis in OpenSim to map assistive cable force to effective lumbar torque assistance for a given trajectory, allowing for intuitive controller design in the lumbar joint space over the complex kinematic chain for varying lifting techniques. Human subject experiments illustrated that the ABX reduced lumbar erector spinae muscle activation during symmetric and asymmetric lifting by an average of 37.8% and 16.0%, respectively, compared to lifting without the exosuit. This result indicates the potential for our device to reduce lumbar injury risk.

Index Terms—Biologically-inspired robots, lifting exosuit, tendon/wire mechanism, wearable robots.

I. INTRODUCTION

A. Overview

OW back pain (LBP) is one of the most prevalent health issues in the United States, causing physical pain, re-

Manuscript received March 24, 2021; revised July 2, 2021; accepted August 22, 2021. This work was supported in part by the National Science Foundation, National Robotics Initiative under Grant 1830215, in part by the National Science Foundation Graduate Research Fellowship under Grant DGE-1650044, and in part by the NSF Research Traineeship: Accessibility, Rehabilitation, and Movement Science (ARMS) under Grant 1545287. This paper was recommended for publication by Associate Editor R. Ozawa and Editor M. Yim upon evaluation of the reviewers' comments. (Corresponding author: Jared M. Li.)

Jared M. Li and Andrew S. King are with the Woodruff School of Mechanical Engineering, Georgia Institute of Technology, Atlanta, GA 30332 USA (e-mail: jaredliwork@gmail.com; kandrew@gatech.edu).

Dean D. Molinaro and Anirban Mazumdar are with the Woodruff School of Mechanical Engineering, Georgia Institute of Technology, Atlanta, GA 30332 USA, and with the Institute of Robotics and Intelligent Machines, Georgia Institute of Technology, Atlanta, GA 30332 USA (e-mail: dmolinaro3@gatech.edu; anirban.mazumdar@me.gatech.edu).

Aaron J. Young is with the Institute of Robotics and Intelligent Machines, Georgia Institute of Technology, Atlanta, GA 30332 USA, and also with the Woodruff School of Mechanical Engineering, Georgia Institute of Technology, Atlanta, GA 30332 USA

This article has supplementary material provided by the authors and color versions of one or more figures available at https://doi.org/10.1109/TRO.2021.3112280.

Digital Object Identifier 10.1109/TRO.2021.3112280

duction in quality of life, and economic hardship [1]–[3]. For example, it has been estimated that LBP costs approximately \$20 billion a year in direct medical expenditures and \$100 to \$200 billion annually when considering indirect costs, such as lost wages due to work absence [4]. Regardless, the prevalence of LBP continues to rise. For instance, Freburger *et al.* [5] conducted a study of North Carolina households in 1992 and 2006, finding that LBP prevalence doubled over the 14-year timeframe.

Manual materials handling (MMH) tasks are a common source of risk for LBP [6] and have been found to be a predictor of LBP in several previous studies [7]-[9]. Biomechanically, the lumbar spine and lumbar muscles are usually indicated as the most affected areas [10]. Trunk extensor muscles, primarily the lumbar erector spinae (LES) groups, generate biological moments to stabilize and extend the spine during lifting [11], [12]. Frequent and high-load MMH activities require the repeated generation of these biological moments. This increases the risk of strain in the erector spinae, prolapse, or protrusion of intervertebral discs from compression and shear in the lumbar spine, and damage to the vertebral joints, which can all contribute to LBP [12], [13]. Though symmetric lifting can inflict this damage, asymmetric lifting involving the twisting of the lumbar spine can exacerbate existing symptoms and increase the risk of LBP [12], [14], [15]. Specifically, twisting during lifting has been shown to reduce available trunk strength by up to 21% [16] and increase compressive and shear loading in the lumbosacral (L5/S1) joint during various MMH tasks [17]-[20]. Despite the increased danger, asymmetric lifting remains present in many MMH occupations [21].

Exoskeleton technology has become an increasingly popular countermeasure to LBP [22]. However, most current devices limit the user's allowable range of motion, provide only unidirectional assistance during multidimensional asymmetric movement, or are unable to modulate assistance based on changes in user needs. Thus, we present the design and quantitative human subject assessment of the Asymmetric Back Exosuit (ABX), an active, cable-driven back assistive device (see Fig. 1). The ABX fundamentally differs from previous devices as it can provide lumbar assistance in multiple degrees of freedom (DoFs) without limiting the user's range of motion. Our validation results show that assistance from the ABX reduced trunk extensor muscle activation during a wide range of lifting techniques and object weights.

1552-3098 © 2021 IEEE. Personal use is permitted, but republication/redistribution requires IEEE permission. See https://www.ieee.org/publications/rights/index.html for more information.

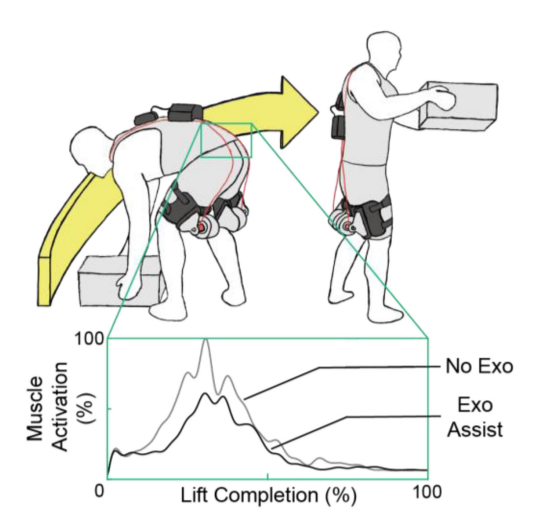


Fig. 1. Asymmetric Back Exosuit (ABX) was designed to assist users during symmetric and asymmetric (shown here) lifting. ABX successfully reduced user lumbar erector spinae muscle activation during lifting compared to lifting without the exosuit. Muscle activations are shown normalized to the peak value of the No Exo condition.

B. Related Work

Industrial exoskeleton technology has the potential to mitigate LBP induced from MMH tasks. As a result, previous research has studied the benefit of applying external mechanical power to the user during lifting through two main categories of assistive devices: passive and active [22], [23]. These devices are often validated by quantifying their effect on trunk muscle activation using electromyography (EMG) [22] due to the known correlation among low back muscle activation, lumbar extensor moment generation, induced lumbar spine compression and shear, and LBP development [12], [24].

Passive devices generally use pliable materials and unpowered actuation to provide passive assistance during lifting [25]-[28]. The soft nature of these systems has yielded devices that are lightweight and allow the user to maintain their natural range of motion. Additionally, the absence of rigid articulated frames eliminates the need for strict actuator colinearity with the joints of interest [29]. These benefits generally make flexible passive devices more suited for asymmetric lifting tasks [27], [30]. However, these benefits come at the cost of fixed assistance based on the mechanical properties of the elastic elements [29]. This decreases the versatility of passive devices when lifting conditions change. For example, assistance magnitude and application style stays constant regardless of object weight or positioning, which are known to change the demands on the biological joints [19], [20], [31]. Also, extreme asymmetric dynamic lifting (e.g., lifting an object with a 180° twist of the trunk) has not been explored [27], [30].

Conversely, active back devices generally utilize rigid frames, powered actuators, and various sensing systems to deliver controllable assistance to the user during lifting [32]–[36]. Common among these designs is high magnitude torque assistance applied at the hips, resulting in a significant decrease of EMG activation of the low back muscles. Though the assistance trajectory and

magnitude can be effectively modulated for changes in task or user needs, these devices present significant drawbacks. For example, the increased weight from powered actuators and large batteries can be cumbersome, and rigid skeletal structures can restrict user range of motion [29]. Additionally, the actuators of active back devices are typically placed in-line with the user's joints, which can lead to parasitic forces that compromise device comfort and assistance controllability if misaligned [29], [37]. Furthermore, the reduction in user range of motion caused by rigidity prevents most active back devices from assisting outside of the sagittal plane, limiting their benefits to symmetric lifting. It is also important to note that time under load should be reduced as integrated lumbar moments are highly correlated with LBP [38]. Therefore, attempting to perform a multidirectional asymmetric lift while physically restricted to one direction by an active device may cause even more harm to the lumbar spine. Though asymmetry has been previously explored in active devices, no biological outcomes were measured [39], and extreme asymmetric movements were not evaluated [34].

It is important to note that, while true in the majority of devices, passive, and active devices are not beholden to flexibility or rigidity. Systems that utilize cable-driven actuation are good examples of this. This technique hybridizes the assistance techniques of passive and active systems since cables function similarly to parallel actuation methods (i.e., elastic elements) [40], [41]. Furthermore, induced moments can be modulated and amplified as needed by powered actuators [40], [41]. This method also allows for greater control authority over complex joint spaces with numerous DoFs [42], [43]. Despite the advantages of cable-driven actuation, very little research has investigated the effects of cable-driven back assistive devices beyond limited symmetric motion [44], [45].

C. Contribution

Neither active nor passive devices have completely addressed the issue of assisting in asymmetric dynamic lifting. Specifically, there is a gap in the field for a device that exhibits the advantageous features of both device types. This involves key design requirements: 1) maintains user freedom of movement; 2) provides active lumbar torque assistance regardless of lumbar kinematics within normal range of motion; and 3) maximizes the likelihood of reducing low back muscle activation. Responding to this gap, we designed, developed, and evaluated the ABX, a novel active exosuit that combines flexible, biologically-inspired actuation common in passive devices, with controllable powered assistance characteristic of active devices. Active force application affords the ABX greater assistance magnitude capability and controllability over passive devices of similar structure. Using cable-driven actuation, the ABX reduces trunk extensor muscle activation of the user in symmetric and extreme asymmetric (90° to 180° twists) lifting, preserves the user's range of motion to promote minimal time under load, and provides assistive torque over the three axes of the lumbosacral joint while keeping the overall device lighter and lower profile relative to active devices of similar capability.

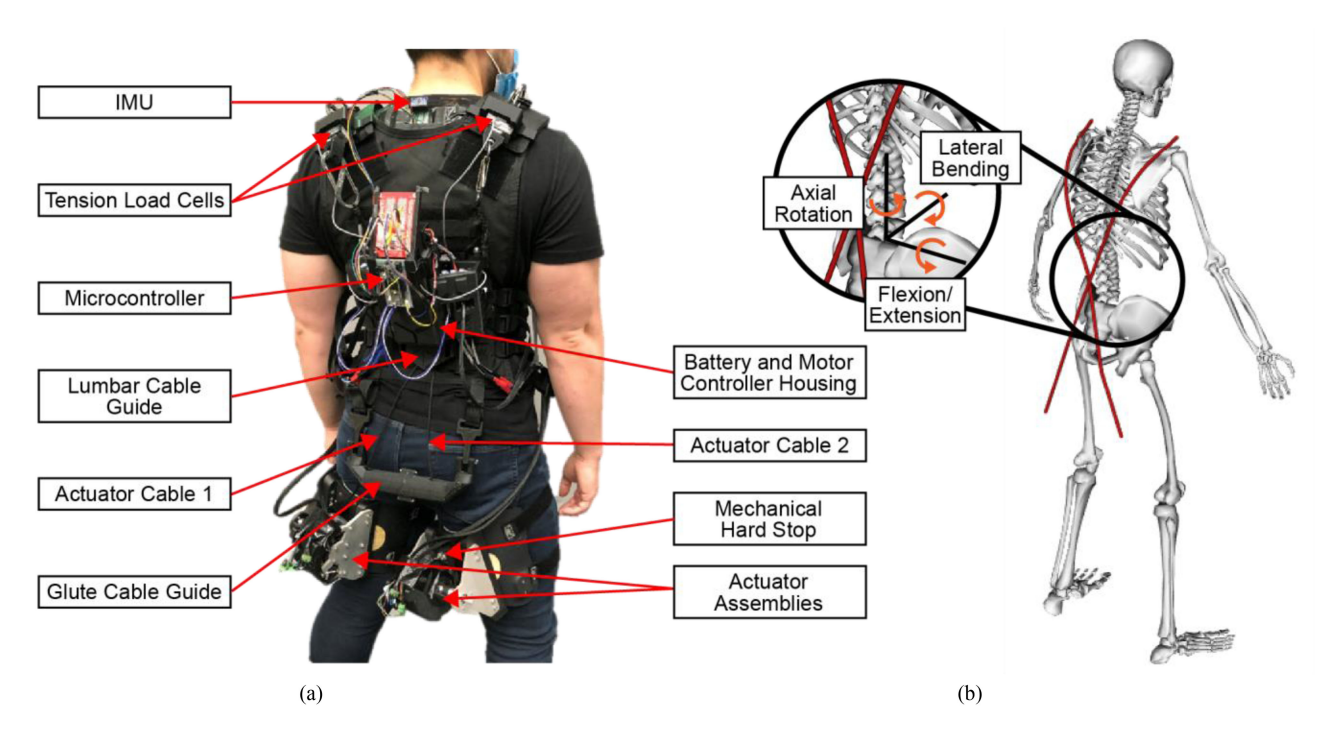


Fig. 2. (a) Asymmetric Back Exosuit (ABX) designed and validated in this article is shown. Thigh-mounted actuators tension the nylon cables attached to opposite shoulders to assist the user during symmetric and asymmetric lifting. Additionally, the microcontroller, batteries, and motor controllers are mounted on the back of the user, making the ABX a fully autonomous system. (b) To characterize the mechanical advantage of the ABX on the lumbar spine, the actuator cables were modeled with respect to the user in OpenSim. As shown, the actuator cables generate an assistive torque in the flexion/extension, axial rotation, and lateral bending degrees of freedom of the lumbosacral joint located at the origin of the lumbar reference frame.

The remainder of this article details the rationale and design of the ABX as specified by our design requirements and includes a validation of the benefits the device has on users during symmetric and asymmetric lifting. Section II details the device conceptualization and physical realization. Section III presents the sensor integration and control system used to autonomously assist the user during lifting. Section IV explains the methods used for human-subject validation of the device. Section V reports the results of these experiments, quantifying both the assistive torque of the device through multiple lifting conditions and the effectiveness of the ABX on preserving user range of motion and reducing trunk extensor EMG. Finally, a discussion of our analyses and final remarks are provided in Sections VI and VII, respectively.

II. EXOSUIT DESIGN AND RATIONALE

A. Exosuit Actuation

We designed the ABX using cable-driven actuation (see Fig. 2), which generates three-DoF assistance via tension, similar to trunk extensor muscle function [41]. This method of actuation ensures ABX can achieve lumbar assistance magnitudes comparable to previous active devices [32]–[36] while maintaining the user's freedom of movement. Cable-driven actuation provides three key benefits over actuators mounted in-line with biological joints for lumbar assistive devices: 1) cable-driven actuation can provide assistance over multiple DoFs (i.e., the intervertebral and hip joints) without adding additional actuators or device joints [43], [45], [46]; 2) unlike

rigid, in-line actuation interfaces, cable-driven systems improve design flexibility since the actuators do not need to be colinear with the biological joint [45]; and 3) with sufficient cable routing, the device actuators can be placed independently of biological joint location [23], [45]–[47], resulting in increased user comfort and offloading of the actuator weight from the lumbar spine. Given these benefits, cable-driven actuation allows the ABX to provide active assistance across the hip and intervertebral DoFs while preserving the user's range of motion. Furthermore, we implemented two independently actuated cables that attach to each of the user's thighs and opposite shoulders, resulting in an "X" pattern crossing along the lumbar spine. This actuation geometry was selected to increase the mechanical advantage of the ABX cables with respect to the lumbosacral axial rotation DoF during asymmetric lifting at the cost of reduced mechanical advantage about the other DoFs. This design choice was made to ensure substantial assistive torque could be generated in the axial rotation DoF, given that the device generates the lowest assistive torque in this DoF compared to flexion/extension and lateral bending (see Section V-C). The actuator placement and resulting simple cable geometry also minimize weight induced on the lumbar spine during lifting and limit friction in cable actuation.

Despite these advantages, cable-driven actuation can result in a reduced mechanical advantage with respect to the lumbosacral joint compared to in-line actuation [32]–[36]. Thus, it was important to design the ABX actuators to generate sufficient cable force to induce lumbar torque assistance magnitudes comparable to that of other active devices. Using a simplified two DoF (hip

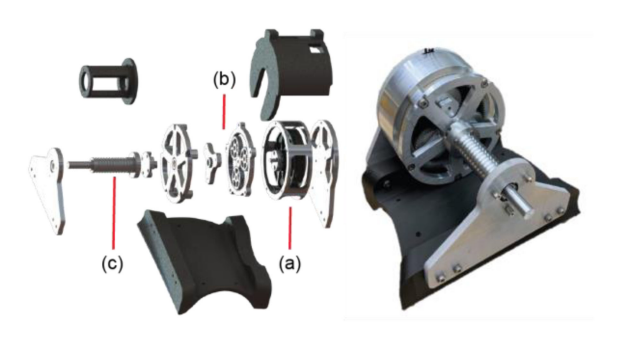


Fig. 3. ABX thigh-mounted actuator is shown. The left subfigure shows an exploded view of the system, where (a) is the brushless dc motor driving the assembly and (b) is the 6:1 planetary gear reduction that transmits torque to the output pulley (c). Depicted above (a) is a plastic motor cover, which routes the motor windings and hall-effect sensor wires away from the cable line of action. Shown above (c) is the cable guide, which encapsulates the pulley in order to enforce proper spooling and prevent cable backlash. Below (b), the orthotic bracket, which fastens the actuator to the thigh orthosis is shown. The assembled actuator is shown to the right of the exploded view.

and lumbar extension) lifting model similar to previous studies [48], [49], we designed our actuators such that the maximum induced lumbosacral extension assistance was larger than 100 Nm, which is approximately 50% of the peak biological moment in unloaded trunk extension [31]. We computed a required tension in each cable (s_m) of 556 N to achieve a lumbar assistive torque (τ_t) of 100 Nm using a moment arm (r_t) of 9 cm [26] as

$$s_m = \frac{\tau_t}{2r_t} \ . \tag{1}$$

Additionally, we computed the maximum expected shortening speed of the cable (\dot{l}_m) to ensure our actuators were not speed limited. Assuming lossless energy transfer between the cable and joint (θ) , the effective moment arm (r_θ) can be expressed using the joint velocity (ω_θ) as

$$r_{\theta} = \frac{\dot{l}}{\omega_{\theta}} \ . \tag{2}$$

Thus, the maximum expected cable shortening speed was computed as 28.7 cm/s using normative hip and lumbar extension velocity trajectories during symmetric lifting [50], assuming constant moment arms of 9 cm for both the hip and lumbar joints using

$$\dot{l}_m = \max \sum_{i}^{n_\theta} r_i \omega_i \ . \tag{3}$$

Using these linear force and speed requirements, we designed and manufactured an actuator assembly for each cable of the exosuit (see Fig. 3). Driving each assembly is a U8-Lite KV100 brushless dc motor (T-Motor, Nanchang, Jiangxi, China), rated to provide 2.42 Nm at 395.5 rad/s, which was further characterized by Lee *et al.* [51] across several operating conditions. The output torque of the motor is amplified by a custom 6:1 planetary gear transmission, which is then converted to linear force by a pulley with an outer diameter of 2.09 cm (0.83 in). The pulley diameter was selected to maximize force output of the actuator while maintaining a sufficient bend radius for the nylon actuation cable [52]. The actuator transmission results in a cable tension

TABLE I SPECIFICATIONS OF BACK ASSISTIVE DEVICES

Device	Туре	Mass (kg)	Trunk Extension Assistance (Nm)		
Lamers et al. (2017)	P	2.0	12		
Toxiri et al. (2018)	A	11.0	80		
Zhang and Huang (2018)	A	11.2	100		
Alemi et al. (2019)	P	4.5	-		
Yong et al. (2019)	A	5.0	128		
Heo et al. (2020)	A	10.5	80		
Koopman et al. (2020)	P	6.7	50		
ABX	A	6.4	172*		

P = Passive, A = Active. * represents peak extension torque at start of the symmetric lift (see Section IV).

of 1385 N given a motor torque of 2.42 Nm, which is larger than the required peak cable tension of 556 N. Additionally, for this torque, the linear speed of the cable is 69.1 cm/s, which is above the minimum target of 28.7 cm/s.

The actuator pulley, housing, and mounting plates were manufactured in-house from aluminum 6061 using CNC. Similarly, the planetary gear transmission was also manufactured in-house from the same material using wire EDM. Ball bearings were mounted on each side of the actuator pulley to offload the axial force from the cable around the gear transmission and motor. The actuators weigh 1.55 kg each, and fully assembled, the ABX weighs a total 6.4 kg, which is substantially less than most previous active devices while having much greater assistive torque capability (see Table I). Despite this, previous research has shown that the average comfort limit of force being applied to the shoulders by cables is around 621 N [53]. This indicates the full assistance capabilities of the ABX are beyond what is generally comfortable to users. Therefore, we chose an assistance magnitude of 25% of the average body weight of an adult male in the United States as a nominal target for actuator performance on the benchtop. For an average weight of around 91 kg (200 lbs) [54], the resulting linear force generation of 222 N across a user's trunk (both cables combined), which is a similar figure to assistance magnitudes used by previous passive devices of similar structure [26], [30].

B. Human Interface

The exosuit attaches to the user's thighs and trunk using orthotic interfaces (Fillauer, Chattanooga, TN, USA) and a supportive modular vest (Condor Outdoor, Irwindale, CA, USA), respectively [see Fig. 2(a)]. The actuator mounting plates attach to the thigh orthosis via a custom-made mounting bracket. To fit the actuator mounting bracket to the custom thigh orthosis, the thigh orthosis was three-dimensional (3-D) scanned using a FaroArm (FARO, Lake Mary, FL, USA), and the mounting bracket was shaped using the generated point cloud.

C. Actuation Cable Routing

To ensure proper spooling of the cable around the actuator pulley, the pulley was externally threaded with a pitch of 0.38 cm. This resulted in a maximum spooling length of 79 cm. Additionally, a cable guide was assembled around the pulley to ensure the cable spooled along the external threads. After the actuator pulley, the cable is routed through the mechanical hard stops, which were made from wire rope clamps used to limit the maximum cable length the actuators can spool [see Fig. 2(a)]. This was used to prevent overextending the user beyond an upright position in the case of unintended device actuation. The cables were then routed through the glute cable guide to ensure that the cables do not slip around the user, which would degrade the lumbar assistive torque of the exosuit. The glute cable guide is adjustable for each user and attaches to the exosuit vest through mesh straps near the low back. The actuation cables then pass through the lumbar cable guide and electronics housing, which facilitates the crossing pattern of the cables. Finally, each cable attaches to the opposite shoulder attachment via a carabiner mounted in series with the tension load cells (see Section III-A). All cable guides were manufactured using an Ultimaker 2+ 3-D printer with Ultimaker Tough PLA (Ultimaker, Utrecht, NL).

III. EXOSUIT INTEGRATION AND CONTROL

A. System Integration

The exosuit controller is executed using a sequential control loop deployed on an onboard Teensy 3.6 (PJRC) microcontroller (MC) at 200 Hz. The exosuit uses two load cells (Transducer Techniques, Temecula, CA, USA), one placed at each shoulder attachment in-line with the actuator cables to measure linear force provided to the user. The load cell output voltages are amplified using two AD623 op-amps (Analog Devices, Norwood, MA, USA) and are each sampled once per control loop. An MPU9250 inertial measurement unit (IMU) (TDK, San Jose, CA, USA) is placed at the cervicothoracic junction, which estimates trunk orientation in real-time as a set of Euler angles updated by the built-in digital motion processor at 67 Hz. Two electronic speed controllers (ESCs) (Flipsky, Dongguan City, China) govern actuator operation using speed control based on serial commands from the MC over UART. The actuators are powered using two 22.2 V, 3600 mAh LiPo batteries (Venom Power, Rathdrum, ID, USA) wired in series. From an estimate of battery life in this configuration, the ABX can provide over two hours of continuous lifting assistance at 111 N for each actuator. The load cells are powered using a separate 11.1 V, 800 mAh LiPo battery (Venom Power, Rathdrum, ID, USA). The MC, ESCs, load cell amplification circuit, and batteries are mounted in the electronics housing located along the user's thoracic spine [see Fig. 2(a)].

B. Finite State Machine

We implement a two-tier control system to autonomously assist the user. Specifically, the mid-level finite state machine (FSM) detects the user mode throughout the lift (see Fig. 4) and updates the control gains and desired cable tension (s_d) of the

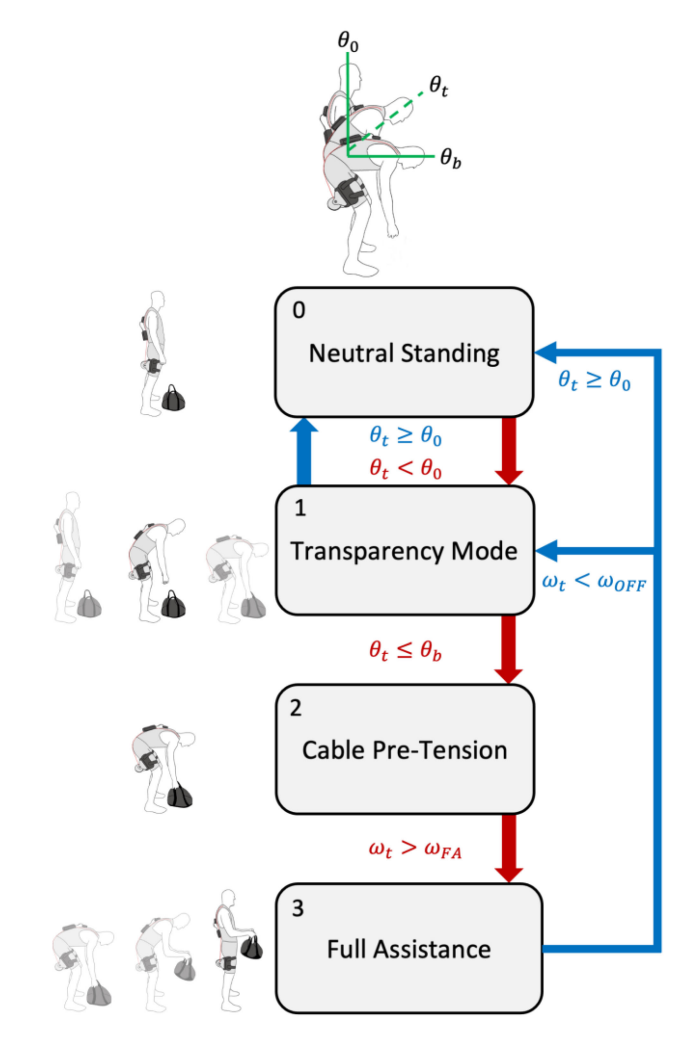


Fig. 4. FSM used to control the ABX is shown. When device operation begins, the user stands in neutral position (State 0). Once they begin to bend their trunk ($\theta_t < \theta_0$) the actuators slack or tension the cables based on the flexion/extension angle of the trunk (State 1) until the user bends down past the bent angle threshold ($\theta_t \leq \theta_b$). The user prepares to lift an object as the cables spool up until the desired assistive force is reached (State 2). Once this occurs, the user initiates full assistance (State 3) by beginning to lift so that their trunk flexion/extension angular velocity is greater than the set threshold ($\omega_t > \omega_{FA}$). Once the user is at the top of the lift and stops moving, the device returns to State 0. If the user stops in the middle of the lift and does not reach neutral standing, they enter State 1.

low-level force controller accordingly. Before device operation, s_d is set to 25% user bodyweight for on-human operation or 111 N for actuator performance evaluation. The low-level control law computes the commanded motor velocity of each motor ($\omega_{\rm cmd}$) using the difference between s_d and the measured cable tension (s) from the corresponding load cell, the measured user trunk extension velocity (ω_t) from the IMU, and the control gains (k_s and k_h) as

$$\omega_{\rm cmd} = k_s \, \left(s_d - s \right) + k_h \omega_t \,. \tag{4}$$

The first term in the control law is used to track the desired cable tension using the proportional gain k_s . The second term is used to compensate for the movement of the user. This allows

the cables to unspool as the user bends down towards the object and provides a convenient method for taking up the slack in the cable as the user lifts the object. This allows the proportional error term to be tuned with a much smaller gain as it is not needed for compensating for user movement, but rather for tracking the desired force using conventional servo control.

The magnitudes of k_s and k_h are hand-tuned for each user to optimize force tracking. Once tuned, these gains are autonomously varied during the lift depending on the user state detected by the FSM, as shown in Fig. 4. The parameters θ_0 and θ_b are defined as the stand angle (the trunk angle measured by the IMU corresponding to when the user is in a neutral standing position) and bent angle (the trunk angle measured by the IMU that occurs $\sim \! 10^\circ$ before the user reaches the bottom of the lift), respectively. These values are also calibrated per user before device operation. Hand-tuning of the control gains and FSM thresholds takes approximately 10 min per subject.

During operation, the FSM transitions between states based on the measured trunk extension angle (θ_t) and trunk extension velocity (ω_t) . Neutral Standing (State 0) is entered when the trunk extension angle is larger than the stand angle $(\theta_t \geq \theta_0)$. During Neutral Standing, the FSM sets k_s and k_h to zero to disable operation of the actuators. The FSM transitions to Transparency Mode (State 1) from Neutral Standing once the trunk extension angle is less than the stand angle $(\theta_t < \theta_0)$. During Transparency Mode, k_s is set to zero and k_h is updated to the tuned magnitude to allow transparent (open-loop zero force) tracking of the cables with the user's trunk motion. Once the user's trunk flexion reaches or exceeds the bent angle $(\theta_t \leq \theta_b)$, the FSM transitions to cable pretension (State 2). During Cable Pre-Tension, k_s and k_h are set to the previously tuned magnitudes and s_d is incremented from zero to the starting assistance force over a 500 ms period. This allows the actuators to preemptively remove slack from the cables and quickly ramp up to assistance while avoiding user discomfort, similar to the action of an elastic element. After tensioning the cables, the FSM transitions the low-level controller into Full Assistance (State 3) once the user's trunk extension velocity exceeds a predefined threshold (ω_{FA}) . For this article, we fixed ω_{FA} at 1.2 rad/s (70 °/s) for all users. During Full Assistance, k_s and k_h remain at their tuned magnitudes to provide assistance according to the programmed desired force trajectory. Once the user's trunk extension angle exceeds the stand angle during Full Assistance, the FSM transitions back to Neutral Standing. Additionally, the FSM is programmed to transition to Transparency Mode if ω_t falls below a predefined threshold (ω_{OFF}) during Full Assistance as an additional safety feature. We fixed this threshold at 0.5 rad/s (30 °/s) for all users. Thus, our exosuit is completely autonomous, meaning that the system hardware is self-contained on the user and that the controller does not require external information (e.g., manual mode transitions).

C. Exosuit Evaluation

To evaluate the performance of our actuators in providing assistive force, steady-state force tracking was evaluated during benchtop and on-user conditions using the previously mentioned

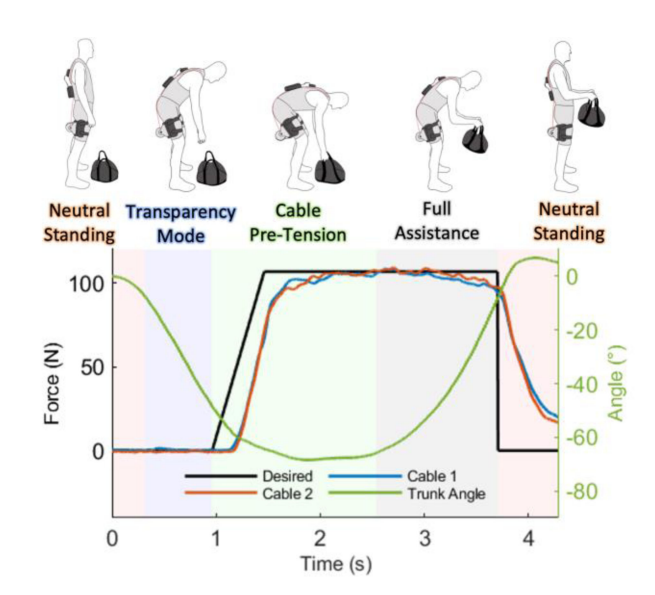


Fig. 5. Representative trial of the actuator performance during on-subject assistance is shown. The phases of the lift are characterized by the background colors on the plot. Desired force is the black profile, and tracking this profile are left and right actuators (blue and red). The flexion/extension angle of the user's trunk is shown in green. During Full Assistance, the actuators tracked the desired force of 111 N (25 lbs.) with an RMSE of 1.8 N.

nominal desired force of 111 N (25 lbs). During the benchtop condition, the actuator was mounted to a screwboard and connected to a tension load cell by a 100 cm nylon cable (approximate maximum cable length during lifting). Desired force was ramped up from 0 to 111 N over 500 ms and the resulting force was measured by the load cell at 200 Hz. The 500 ms ramp time was selected to maximize user comfort during cable pretension while reducing the time necessary to stay bent over. The same protocol was performed using both the left-thigh and right-thigh actuators. Additionally, we tested the ABX assistance tracking performance while worn by a human subject lifting a 15.9 kg (35 lbs.) weighted bag. Similar to the benchtop condition, the desired force was increased from 0 to 111 N per cable over 500 ms during cable pretension and commanded to a constant desired force of 111 N during Full Assistance. The steady-state force tracking error for the benchtop condition was computed as the root-mean-square error (RMSE) between the desired and measured cable force over the first two seconds after the cable reached 95% of the 111 N desired force. Similarly, the force tracking error for the on-subject condition was computed as the RMSE between desired and measured cable force during Full Assistance. The on-subject assistance was controlled using the autonomous FSM.

During the benchtop condition, the average assistance tracking RMSE was 2.4 and 1.4 N for the left-thigh and right-thigh actuators, respectively. Fig. 5 shows a representative trial during the on-subject condition. Like the benchtop condition, the assistance tracking RMSE during the on-subject condition was 1.2 ± 0.4 N and 2.3 ± 0.8 N for the left-thigh and right-thigh actuators, respectively. In both conditions, the average tracking RMSE was less than 3% of the total desired force, demonstrating that the actuators accurately provided cable tension.

IV. HUMAN-EXOSUIT OUTCOMES VALIDATION

A. Overview

We conducted a series of experiments to evaluate the effect of the ABX assistance on user outcomes. Specifically, we measured the change in EMG measurements of the trunk musculature compared to lifting without the exosuit to quantify the benefits of the ABX on reducing low back muscle effort. Additionally, we measured lumbar range of motion (RoM) with and without the exosuit to assess any penalties the ABX may have on the user's freedom of movement. Finally, we adapted a previously validated full-body OpenSim model [55]-[57] to quantify the assistive workspace of the exosuit with respect to the lumbosacral joint. This third analysis provided a high-fidelity characterization of the ABX's effect on the three-DoF lumbosacral moments, relaxing the assumptions and limitations of previous back assistive device analyses, such as assuming constant device moment arms and planar lumbar movement [26], [48], [49]. Lumbar dynamics are reported as defined by the lumbosacral reference frame shown in Fig. 2(b).

B. Experimental Protocol and Measurements

To evaluate the effects of ABX assistance on the user during lifting, we conducted a three subject (average age of 22.7 \pm 0.6 years, mass of 79.1 \pm 3.6 kg, and height of 1.79 \pm 0.06 m) validation experiment approved by the Georgia Institute of Technology Central Institutional Review Board (H19276). Each subject provided informed consent prior to completing the experimental protocol, and none of the subjects had histories of low back injury or musculoskeletal disorders that would confound the results of this experiment. The participants lifted weighted bags using three techniques, which were labeled the symmetric (SYM), asymmetric 90° (ASYM90), and asymmetric 180° (ASYM180) techniques, designed to vary the lumbar twist at the start and end of the lift (see Fig. 6). Each lifting technique consisted of lifting the weighted bag from the ground (\sim 5 cm away from the user's feet) and placing it on a table with a height of 75 cm. The SYM technique consisted of sagittally lifting the weighted bag from a starting position directly in front of the user's feet and ending directly in front of the user. The ASYM90 technique involved lifting the weighted bag placed on the user's right side to enforce a 90° rotation at the start of the lift and placing the bag on the table directly in front of the user. Finally, the ASYM180 technique involved lifting the weighted bag placed on the user's right side and placing it on the table set on the left side of the user, inducing a 180° rotation from the start to end of the lift. Each participant completed five repetitions, lifting three different weighted bags of 6.8, 15.9, and 22.7 kg (15, 35, and 50 lbs., respectively) for the SYM and ASYM90 techniques and lifting a single weighted bag of 15.9 kg (35 lbs.) for the ASYM180 technique under two exosuit conditions. The exosuit conditions were: 1) NO EXO, in which the user completed the lifts without wearing the exosuit, and 2) EXO ASSIST, in which the exosuit actively provided 25% of the user's bodyweight evenly distributed between the cables during the upward portion of the lift, similar to the peak assistance force in a previous

SYM





ASYM90





ASYM180





Fig. 6. Experimental setup is shown. The participants lifted weighted bags of 6.8, 15.9, and 22.7 kg (15, 35, 50 lbs.) from the ground to a 75 cm elevated table using varying lifting techniques. The symmetric (SYM), asymmetric 90° (ASYM90), and asymmetric 180° (ASYM180) lifts were tested to evaluate the effects of exosuit assistance across common lifting techniques of varying lumbar twist.

passive garment study [26]. Thus, each subject completed 70 lifting repetitions. While lift timing was not explicitly controlled, each lift was recorded over a three second period. This provided enough time for participants to initiate lifting, place the bag on the elevated table, and return to neutral standing position. Prior to completing the experimental conditions, participants were instructed to stand with feet shoulder-width apart and to stoop while lifting with a slight bend in the knees across lifting techniques. The movements were practiced across bag weights and lift techniques until the participants were comfortable with the movements and proper lifting technique was verified by the experimenters.

During each experiment, electromyography (EMG) data were collected using a Biometrics DataLINK DLK900 Data Acquisition System (Biometrics Ltd, Newport, U.K.) at 1000 Hz. Electrodes were placed on the left and right lumbar erector spinae (LLES and RLES), left and right latissimus dorsi (LLD and RLD), left and right external obliques (LEO and REO), and rectus abdominis (RA) muscle groups. The electrodes were placed on the skin surface in accordance with SENIAM standards [58], which outline the optimal location and orientation

of the EMG electrodes for each muscle group. Proper electrode placement was verified by visual inspection while asking the participants to activate each muscle group.

On a separate day, one participant (age of 23 years, mass of 81.6 kg, and height of 1.75 m) returned to complete a second experimental protocol to collect kinematic data to evaluate user range of motion changes when using the ABX. The second protocol consisted of seven lifting repetitions of the 15.9 kg (35 lbs.) bag using each of the three prescribed lifting techniques. During this protocol, the NO EXO and EXO ASSIST conditions were repeated, as well as a SLACK condition, in which the exosuit was worn while unpowered with slack in the cables during the entire lift. During this experiment, whole-body motion capture data was collected using a 32-camera Vicon motion capture system (Vicon, Oxford, U.K.) at 200 Hz. Retroreflective markers were used to collect kinematic data of the feet, shanks, thighs, pelvis, trunk, arms, and hands. Additionally, to mark the start and end timing of lifting the weighted bag, six-axis force data were collected using two Bertec force plates (Bertec, Columbus, Ohio, USA) at 1000 Hz. One was placed next to the user on the ground, while the other was placed on the elevated table.

Between every repetition of experimental conditions for both experimental protocols, participants rested for around 30 s. After the full set of repetitions per condition were completed, participants rested for one minute while experimental conditions were changed. Finally, a five-minute rest period was enforced with each change in lift technique (SYM, ASYM90, ASYM180). The order of lift technique and bag weight were randomized for both experiments.

C. Exosuit OpenSim Model

To compute the resulting lumbar RoM and assistive torque workspace of the ABX, we modified the OpenSim Lifting Full-Body (LFB) model [57], a musculoskeletal model validated for analyzing the lumbar spine during lifting movements, to include musculotendon actuators representative of the two actuation cables of the ABX [see Fig. 2(b)]. The start and end points of the modeled cables were fixed using the ABX thigh and shoulder attachment locations as measured using motion capture markers during a subject-specific calibration trial. Additionally, the modeled cables were guided along the trunk and pelvic bodies using massless, frictionless wrapping surfaces to mimic the constraints of the exosuit cable guides.

D. Data Analysis

EMG data of each trial were offset by the mean of the signal, filtered using a band-pass 30 to 300 Hz zero-phase fifth order Butterworth filter, rectified, and then low-pass filtered with a 6 Hz zero-phase fifth order Butterworth filter in accordance with standard practices [59]. The root mean square muscle activation (rEMG) was computed over the previously mentioned three second period used to capture each repetition in entirety. The rEMG data for each channel (one per muscle group) of the EXO ASSIST trials were then averaged over the five repetitions per permutation of experimental conditions and then normalized to

the corresponding averaged rEMG data of the NO EXO condition following the same process. The EMG results are presented as the percent change in rEMG of the EXO ASSIST conditions relative to the corresponding NO EXO conditions [average \pm 1 standard error of the mean (SEM)]. One subject's data for the LLES and RLES groups across all conditions were excluded due to malfunction caused by the cable action interfering with the electrodes. Also, for the same subject, EMG malfunction on the RA group occurred during two repetitions of the ASYM90 6.8 kg lifts, which were also excluded.

The motion capture and force plate data were lowpass filtered using a zero-lag fifth order Butterworth filter with a cutoff frequency of 6 Hz and 20 Hz, respectively. The start of the lift was marked when the weighted bag was fully removed from the starting force plate. Similarly, the end of the lift was marked when the weighted bag first contacted the ending force plate. We then computed the lumbar RoM and ABX assistive torque workspace using OpenSim [55], [56]. The motion capture data of the 58-marker full-body marker set was used to scale the anthropometry, inertial properties, and exosuit cable attachment points of the modified LFB model to fit that of the individual participant using the OpenSim Scale Tool. The generalized joint coordinate trajectories of the scaled model for each lifting trial were then computed using the built-in OpenSim Inverse Kinematics Tool, which minimizes the weighted sum of least squares between the experimental and modeled markers as a function of the generalized coordinates of the model. Using these joint trajectories, the lumbar RoM for each trial was computed as the difference between the maximum and minimum trunk angle with respect to the sacrum through the lift in the flexion/extension, axial rotation, and lateral bending DoFs.

We then used the OpenSim Muscle Analysis Tool to compute the ABX moment arms of the scaled model with respect to the lumbosacral joint. The Muscle Analysis tool defines the effective moment arm $(r_{\theta} \in \mathbb{R})$ between a DoF (θ) and musculotendon actuator (a) as the ratio of torque induced at the DoF (τ_{θ}) with respect to the tension force of the musculotendon actuator (s_a) given the set of generalized coordinates of the model (q) [60] as

$$r_{\theta}\left(q\right) \stackrel{\Delta}{=} \frac{\tau_{\theta}}{s_{a}} \ . \tag{5}$$

With this formulation, the solver computes the effective moment arms using two assumptions: 1) the path of the musculotendon actuator (l) is fully described by the generalized coordinates of the model (l = l(q)), and 2) the tension in the musculotendon actuator is uniform and the transform between spatial forces and tension is linear. Using these assumptions, the effective moment arm of the musculotendon actuator is computed using the generalized forces (f(s)) defined by the model geometry, the joint-specific geometric coupling matrix (C_{θ}) , and by fixing s to unit tension (s_{θ}) [60]

$$r_{\theta} = \frac{f^T C_{\theta}}{s_o} \ . \tag{6}$$

The assistive torque workspace of a given biological DoF (W_{θ}) was then computed using the definition show in (5), the effective moment arms of the exosuit cables (R_{θ}) , and the

interval between the minimum (S_{MIN}) and maximum (S_{MAX}) cable tensions that can be generated by the exosuit

$$W_{\theta} (q) = \left\{ R_{\theta}^{T} (q) S \mid S \in [S_{\text{MIN}}, S_{\text{MAX}}] \right\} . \tag{7}$$

Additionally, we defined the maximum restorative torque (J_{θ}) of the exosuit as the maximum assistive torque about a given biological joint that can be generated in the direction of the velocity of the generalized coordinate for the given joint of interest, calculated as

$$J_{\theta} \stackrel{\Delta}{=} \begin{cases} \max \left(W_{\theta} \left(q \right) \right) & \text{if } \dot{q}_{\theta} > 0 \\ \left| \min \left(W_{\theta} \left(q \right) \right) \right| & \text{if } \dot{q}_{\theta} < 0 \\ 0 & \text{otherwise.} \end{cases}$$
 (8)

V. VALIDATION RESULTS

A. Trunk Muscle Activation

Fig. 7 shows the relative change in rEMG of the EXO ASSIST condition compared to the NO EXO condition for each lift technique and weighted bag mass. Across all technique types and bag weights, trunk extensor muscle (LLES, RLES, LLD, RLD) rEMG was decreased. Specifically, with regard to the LLES and RLES groups, large rEMG reductions were observed in symmetric lifting across bag weights (44.0 \pm 3.88% L and $46.5 \pm 3.39\%$ R for 6.8 kg, $36.9 \pm 8.21\%$ L and $37.9 \pm 2.25\%$ R for 15.9 kg, $31.6 \pm 15.6\%$ L and $30.1 \pm 8.38\%$ R for 22.7 kg). Regarding ASYM90 lifting, reductions were also observed, but to a lesser extent (32.0 \pm 6.48% L and 21.0% \pm 20.4% R for 6.8 kg, $6.73 \pm 6.48\%$ L and $14.7 \pm 17.6\%$ R for 15.9 kg, $1.5 \pm$ 6.04% L and $17.8 \pm 10.4\%$ R for 22.7 kg). For the ASYM180 condition, similar reductions are observed (18.0 \pm 15.5% L and $10.2 \pm 16.9\%$ R for 15.9 kg). The LLD and RLD groups also experienced generally large reductions across all conditions and weights, except for the ASYM90 technique with 6.8 kg bag weight.

As for the flexor muscles (LEO, REO, RA), decreases of activation were observed, except for the LEO group at the 6.8 kg bag weight, where activation increased by $12.8 \pm 9.93\%$, during symmetric lifting. Regarding ASYM90, increases of the REO and RA groups of $8.39 \pm 9.69\%$ and $32.6 \pm 34.8\%$, respectively, for the 6.8 kg weight were observed. Another increase occurred for the RA group of $3.79 \pm 5.99\%$ during the 22.7 kg lift of the same technique type. During the ASYM180 technique, RA also increased by $5.31 \pm 0.74\%$. Other than these increases, trunk flexor muscle rEMG was generally decreased across technique types and bag weights.

B. Lumbar Range of Motion

The resulting RoM data are shown in Table II. Lumbar flexion RoM increased by 19.5%, 33.7%, and 6.3% during the SLACK condition and by 33.1%, 39.1%, and 19.2% during the EXO ASSIST condition compared to the NO EXO condition for the SYM, ASYM90, and ASYM180 techniques, respectively. Additionally, the EXO ASSIST condition increased the axial rotation RoM by 0.3° during the ASYM90 technique but reduced the axial rotation RoM by 9.4° during the ASYM180

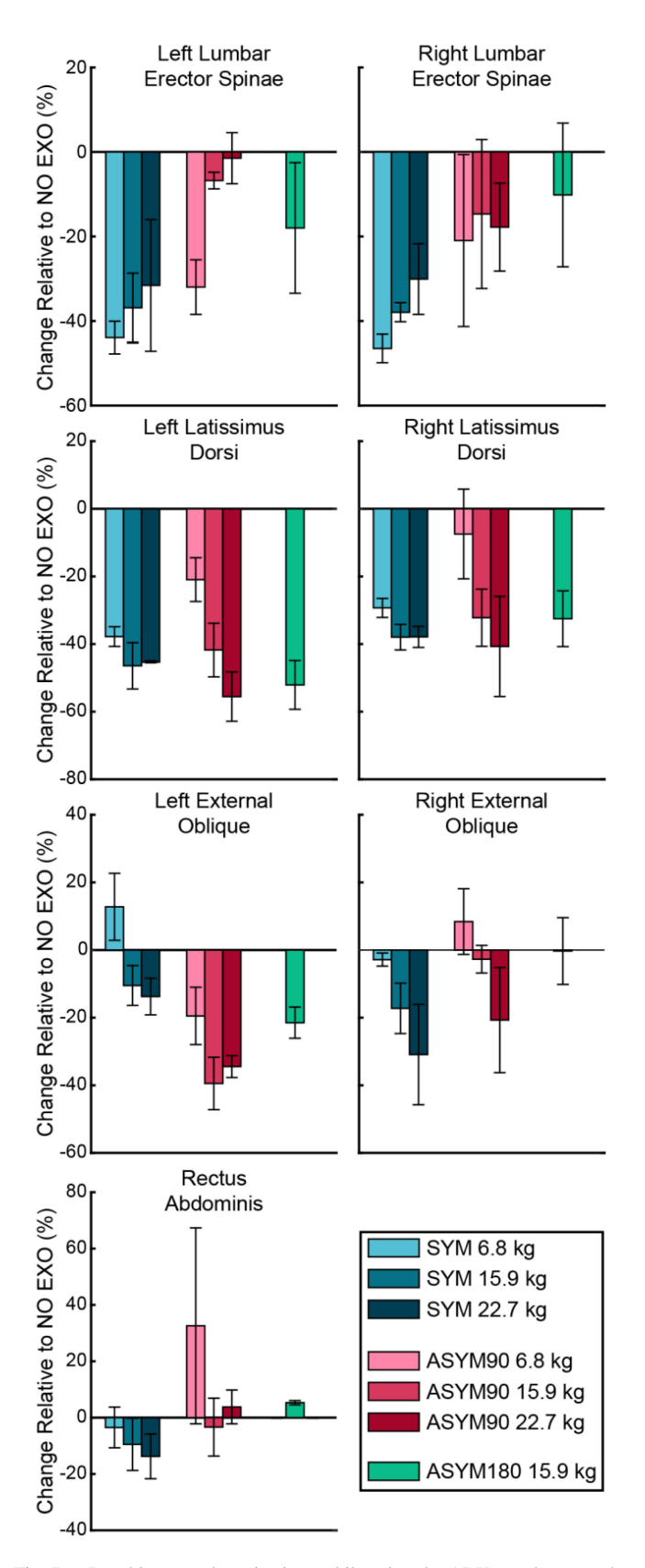


Fig. 7. Resulting muscle activations while using the ABX are shown as the relative change to those measured without wearing the device (NO EXO). All muscle activations were measured using surface electromyography. The results are presented for each tested bag weight during the SYM, asymmetric 90° (ASYM90), and asymmetric 180° (ASYM180) lifts as the average change in rms muscle activation \pm 1 SEM.

10 IEEE TRANSACTIONS ON ROBOTICS

TABLE II LUMBAR RANGE OF MOTION

	Symmetric			Asymmetric 90°			Asymmetric 180°		
	NE	S	EA	NE	S	EA	NE	S	EA
FE	50.7°	60.6°	67.5°	43.2°	57.7°	60.1°	50.0°	53.0°	59.4°
AR	11.0°	4.5°	5.2°	10.1°	13.6°	10.4°	29.7°	29.7°	20.3°
LB	6.6°	3.8°	5.9°	30.2°	27.9°	37.9°	48.3°	38.8°	45.2°

$$\label{eq:FE} \begin{split} FE &= Flexion/Extension, AR = Axial \ Rotation, LB = Lateral \ Bending. \\ NE &= NO \ EXO, S = SLACK, EA = EXO \ ASSIST. \end{split}$$

technique compared to the NO EXO condition. Similarly, for the EXO ASSIST condition, lateral bending RoM increased by 7.7° during the ASYM90 technique but decreased by 3.1° during the ASYM180 technique compared to the NO EXO condition.

C. Lumbar Assistive Torque Workspace

The average lumbosacral extension moment arm of the ABX cables during the SYM lift was 6.73 ± 0.06 cm. Similarly, the averaged extension moment arm was 6.74 ± 0.16 cm and 6.69 ± 0.07 cm during the ASYM90 and ASYM180 lifts, respectively. The axial rotation moment arms varied substantially between cables, resulting in average values of -0.73 ± 0.05 cm, -0.57 ± 0.06 cm, and -0.5 ± 0.07 cm for the left cable and 0.60 ± 0.04 cm, 0.84 ± 0.02 cm, and 0.81 ± 0.05 cm for the right cable during the SYM, ASYM90, and ASYM180 techniques, respectively. Similarly, the average lateral bending moment arms were 1.68 ± 0.09 cm, 0.33 ± 0.18 cm, and 0.44 ± 0.16 cm for the left cable and -1.45 ± 0.05 cm, -2.00 ± 0.14 cm, and -1.75 ± 0.08 cm for the right cable during the three lifting techniques.

The effective workspace of the ABX with respect to the lumbosacral joint over the kinematic trajectory for each of the three lifting techniques is shown in Fig. 8. The maximum restorative lumbosacral torque induced by the device varied throughout the lift. At the beginning of the lift, the maximum restorative torque was 172.4 \pm 4.2 Nm, 165.4 \pm 1.5 Nm, and 163.8 \pm 4.2 Nm in extension, 4.1 \pm 0.9 Nm, 16.2 \pm 0.3 Nm, and 18.3 \pm 3.1 Nm in axial rotation, and 16.4 \pm 1.4, 61.6 \pm 1.7 Nm, and 63.4 \pm 5.1 Nm in lateral bending for the SYM, ASYM90, and ASYM180 techniques, respectively.

VI. DISCUSSION

This article presented the design and human-subject validation of the ABX, an active, cable-driven back assistive device designed for realistic lifting conditions. We designed the ABX to provide active assistance across all DoFs of the lumbar spine while preserving the user's original range of motion during symmetric and asymmetric lifting. Our exosuit uses two cable-driven actuators that generate tension between the user's thighs and opposite shoulders, making an "X" pattern. Each actuator was validated to have an assistance tracking RMSE of less than 3% of the desired cable force. Using a nominal force of 12.5% bodyweight in each actuation cable, we measured reductions in lumbar erector spinae rEMG, ranging from 9.7% to 45.3% on average across bag weights and lifting techniques (see Fig. 7). Importantly, we did not measure increases in antagonist muscle

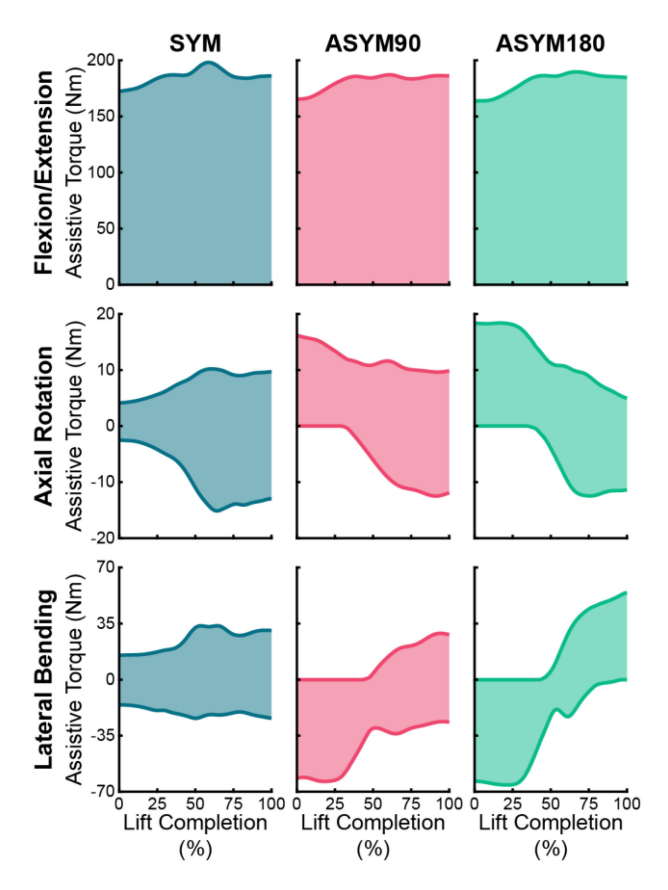


Fig. 8. Averaged assistive workspace of the exosuit, defined as the set of torque values the exosuit can induce on a given degree of freedom for a set of generalized model coordinates, is shown for each lumbosacral degree of freedom (rows) and lifting technique evaluated in our study (columns). The depicted time series start at the bottom of the lift and end when the user placed the weighted bag on the table.

groups (e.g., EO and RA muscles during SYM lifts and REO and RA muscles during ASYM lifts) for most of the lifting conditions, which suggests that the users accepted the device assistance instead of resisting the device by coactivating the antagonistic muscle groups during lifting. Conversely, for the conditions in which this is not true (conditions where trunk flexor muscle EMG increases), it is possible that users had difficulty accepting assistance. This occurred only during the lightest bag weights, meaning that assistance from the ABX may have been too large, resulting in users resisting the device. Additionally, we found that the relative reduction of the erector spinae muscles compared to the NO EXO condition decreased as bag weight increased. Due to the limited number of subjects and high variability in the EMG data, further investigation is needed to validate this result. However, it suggests that exosuit assistive torque should be increased as the lumbar demand increases with bag weight.

The relative reductions in lumbar muscle activation during symmetric lifting in our article are comparable to those reported in previous active back device studies (\sim 25 to 40% in previous studies) [33]–[36], outperforming the results of passive devices (\sim 14 to 29%) [25]–[27] due to the net positive work provided by the ABX. This result demonstrates that the flexible, cable-driven

actuation of the ABX maintains lumbar assistance benefits compared to previous rigid devices.

Furthermore, the flexible nature of the ABX allowed our study to expand the investigation of active lumbar assistance effects on asymmetric lifting with up to 180° of rotation, which previous rigid devices can restrict the user from performing. During the ASYM90 and ASYM180 techniques, the ABX assistance resulted in a relative reduction in lumbar erector spinae muscle activation by an average of 15.6% and 14.1%, respectively, compared to the NO EXO condition. These results are slightly lower in magnitude than passive device results in the literature (24 to 30%) [27], [30]; however, this is likely due to differences in the specific lifting conditions, making direct comparisons challenging. Regardless, the results of our study show that the ABX provides benefits in reducing lumbar muscle activation during symmetric lifting comparable to state-of-the-art active devices but generalizes those benefits beyond the operational workspace of these prior devices with rigid structures.

To characterize the assistance torque delivered to the lumbosacral joint by our exosuit, we adapted a previously validated OpenSim model to include the ABX cables as musculotendon actuators. From this model, we computed the effective moment arms and assistance torque workspace achieved by our device during the three lifting techniques. Interestingly, the average extension moment arm ranged from 6.69 to 6.74 cm among the lifting techniques with little variance throughout the lift (see Fig. 8). This demonstrates that the lumbosacral extension moment arm of the exosuit remained mostly constant through a wide range of lifting asymmetry, which validates the constant extension moment arm assumption common to previous back assistive devices in the literature [26], [48], [49]. Additionally, the resulting lumbosacral extension moment arms of our OpenSim analysis were smaller than originally assumed (see Section II-A); however, they are approximately 50% larger than the moment arms of the erector spinae muscles reported in a comparable musculoskeletal models [57], [61], demonstrating the increased mechanical advantage of the ABX compared to the human musculoskeletal system with respect to the lumbosacral joint.

Using these computed moment arm trajectories and the peak force of our actuators, we computed the assistive torque workspace of each lumbosacral rotational DoF (see Fig. 8). Though we implemented a control reference signal of constant force regardless of lift technique, trunk extension, and bag weight to validate the ABX in this article, future research will include using these workspaces to design optimized assistance trajectories as influenced by changes in lumbosacral joint demands across varying tasks. Additionally, we quantified the maximum restorative torque at each lumbosacral DoF using the assistive torque workspaces. The maximum extension assistance of our device is larger than previous active back devices (see Table I), providing the potential to explore novel magnitudes of actuator assistance, especially given the likely need for increased assistance with increased biological joint demand from varying conditions (i.e., changes in object weight).

We also quantified the user's lumbar RoM during the three lifting techniques investigated in this article. This analysis serves to only validate that the ABX did not inherently limit the user's lumbar RoM, as the low subject count (N = 1) makes it difficult to draw conclusions about intercondition RoM differences. However, we did observe some interesting kinematic effects, specifically the large RoM reduction of 9.4° between the EXO ASSIST and NO EXO condition in axial rotation during the ASYM180 technique. Interestingly, this reduction did not occur during the SLACK condition, suggesting that assistance application was the contributing factor, not restrictions caused by wearing the device itself. The RoM experiment did not result in other evidence that the ABX reduced lumbar RoM during symmetric or asymmetric lifting techniques. Additionally, nonzero axial rotation and lateral bending RoMs were both present in the symmetric lifting conditions, which aligned with previous literature [17]. With increased subject count, the data should become more varied to account for differing postures between subjects.

Though our device performed well in all of the evaluated human subject outcomes, there are a few limitations in the design that should be considered for improving its usefulness. While the ABX is a fully autonomous device, the main issue that limits use in nonexperimental settings is the 500 ms ramp up time. During experiments, this ramp up time was similar to the amount of time needed for the user to finish bending down and to grasp the weighted bag; however, it is possible that this could reduce assistance benefits if the user lifted very slowly or quickly. In the future, this 500 ms ramp up condition could be eliminated by improved cable slack management or anticipated using an intent recognition system and/or EMG measurements. Another limitation is that, based on our OpenSim model, the exosuit cables have a smaller extension moment arm than other devices that use similar actuation methods (e.g., Abdoli et al. [30] reported an extension moment arm of 22 cm using a glute plate). It is likely that the mechanical advantage of our device relative to the trunk extensor muscle groups can also be increased using similar geometric structures. An argument can be made, however, that linear force applied to the lumbar spine regardless of method can cause compression, especially at high force magnitudes. Because the design of the ABX employs larger moment arms than the trunk extensor muscles by a substantial amount with regard to the lumbar spine, it is assumed that the overall joint reaction loads in the lumbar spine are reduced if trunk extensor muscle activation is reduced and trunk flexor muscle activation is either reduced or remains unaffected. However, further analysis is required to validate the assumed correlation between trunk extensor EMG reduction and lumbar spine loading.

Another limitation of our device is that multiple users reported discomfort from the thigh actuators. Mainly, the actuators needed to be fastened tightly to the thighs to hold them in place, which caused user discomfort after prolonged use of the device. This design choice was made to reduce exosuit weight borne on the lumbar spine and to minimize friction in cable routing; however, the actuator placement and mounting should be reconsidered in future modifications to improve comfort and reduce distance from the user's center of mass to save energy while ambulating. Given the maximum actuation force of the ABX is well above previously found comfort limits [53]

and could cause undesired spinal compression if reached, the actuator assistance capability and weight can likely be reduced. Finally, the planetary gearset was manufactured from aluminum 6061, which could result in wear from long term cyclic loading. Though we did not observe any deformation in the transmission system, the longevity of the actuators could be improved by implementing an alternative material.

Our study also included experimental limitations, first, the initial validation of our device presented in this article was limited in subject count for both the EMG analysis (N = 3)and all other human-subject tests (N = 1). Because of this, we lack statistical power to claim significance of results from either experiment. To do so, the experimental subject pool should be increased in size. Additionally, the evaluation of human-subject lumbar benefit was limited to muscle activation results based on trunk EMG. Though this approach has been the standard for evaluating back assistive devices, it does not provide direct insight into the effect the device has on known LBP risk factors, such as compressive and shear loading in the lumbar joints [38]. Future analyses should include quantifying the impacts of our device on LBP risk factors, such as quantifying the change in joint reaction loads using musculoskeletal modeling with a larger cohort of subjects. Another limitation of this article is that we tested only one exosuit assistance magnitude and profile. Though this approach resulted in reduction of trunk extensor EMG for our experimental population, the reference signal used to control the exosuit can likely be optimized further to account for specific three-DoF torque profiles in the ABX's lumbar spine workspace, which leaves the opportunity for increased exosuit benefit in future work. This article was also limited in evaluating only lifting and not lowering. While lifting generates more EMG activation in the erector spinae [62], previous literature indicates that lowering and lifting have differing negative effects on the lumbar spine [63]. For example, lowering induces more compressive force than lifting, while lifting causes more shear force. Therefore, to fully account for mitigating danger to the lumbar spine, future studies with the ABX should also include lowering motions. This is an exciting line of research for our device given that its active nature allows further research to investigate the effects of changing assistance delivery on user benefits.

VII. CONCLUSION

We designed the ABX to actively assist the lumbar spine during symmetric and asymmetric MMH tasks. The ABX uses two independently controlled, cable-driven actuators to assist each degree of freedom of the lumbar spine without limiting the user's range of motion. Our N=3 validation tests showed that the ABX not only reduced the activation of trunk extensor muscles by amounts similar to active devices [33]–[36], but also provided benefits during asymmetric lifting due to its cable-driven design, a novel concept for active back assistive devices. Additionally, the ABX had similar trunk extensor EMG reduction benefits as other passive devices during asymmetric movements, but added benefit during symmetric lifting [27], [30]. While we used a simplified assistance strategy in this article, our lumbosacral

assistive torque workspace can be used for future design of optimized assistance profiles.

REFERENCES

- [1] D. Hoy, P. Brooks, F. Blyth, and R. Buchbinder, "The epidemiology of low back pain," *Best Pract. Res. Clin. Rheumatol.*, vol. 24, no. 6, pp. 769–781, Dec. 2010, doi: 10.1016/j.berh.2010.10.002.
- [2] H. Yang, S. Haldeman, M.-L. Lu, and D. Baker, "Low back pain prevalence and related workplace psychosocial risk factors: A study using data from the 2010 national health interview survey," *J. Manipulative Physiol. Therapeutics*, vol. 39, no. 7, pp. 459–472, Sep. 2016, doi: 10.1016/j.jmpt.2016.07.004.
- [3] A. Wu et al., "Global low back pain prevalence and years lived with disability from 1990 to 2017: Estimates from the global burden of disease study 2017," Ann. Transl. Med., vol. 8, no. 6, pp. 1–14, Mar. 2020, doi: 10.21037/atm.2020.02.175.
- [4] J. N. Katz, "Lumbar disc disorders and low-back pain: Socioeconomic factors and consequences," *JBJS*, vol. 88, pp. 21–24, Apr. 2006, doi: 10.2106/JBJS.E.01273.
- [5] J. K. Freburger et al., "The rising prevalence of chronic low back pain," Arch. Intern. Med., vol. 169, no. 3, pp. 251–258, Feb. 2009, doi: 10.1001/archinternmed.2008.543.
- [6] J. I. Kuiper, A. Burdorf, J. H. A. M. Verbeek, M. H. W. Frings-Dresen, A. J. van der Beek, and E. R. A. Viikari-Juntura, "Epidemiologic evidence on manual materials handling as a risk factor for back disorders: A systematic review," *Int. J. Ind. Ergonom.*, vol. 24, no. 4, pp. 389–404, Aug. 1999, doi: 10.1016/S0169-8141(99)00006-2.
- [7] D. B. Chaffin and K. S. Park, "A longitudinal study of low-back pain as associated with occupational weight lifting factors," *Amer. Ind. Hyg. Assoc. J.*, vol. 34, no. 12, pp. 513–525, Dec. 1973, doi: 10.1080/0002889738506892.
- [8] U. Latza, A. Pfahlberg, and O. Gefeller, "Impact of repetitive manual materials handling and psychosocial work factors on the future prevalence of chronic low-back pain among construction workers," *Scand. J. Work. Environ. Health*, vol. 28, no. 5, pp. 314–323, 2002.
- [9] P. Coenen et al., "The effect of lifting during work on low back pain: A health impact assessment based on a meta-analysis," Occup. Environ. Med., vol. 71, no. 12, pp. 871–877, Dec. 2014, doi: 10.1136/oemed-2014-102346.
- [10] S. M. McGill, "The biomechanics of low back injury: Implications on current practice in industry and the clinic," *J. Biomech.*, vol. 30, no. 5, pp. 465–475, May 1997, doi: 10.1016/S0021-9290(96)00172-8.
- [11] J. R. Potvin, R. W. Norman, and S. M. McGill, "Reduction in anterior shear forces on the L4L5 disc by the lumbar musculature," *Clin. Biomech.*, vol. 6, no. 2, pp. 88–96, May 1991, doi: 10.1016/0268-0033(91)90005-B.
- [12] J. Hamill, K. Knutzen, and T. Derrick, Biomechanical Basis of Human Movement, 4 ed. Philadelphia, PA, USA: Wolters Kluwer Health, 2014.
- [13] M. R. Bracko, "Can we prevent back injuries?," ACSMs Health Fitness J., vol. 8, no. 4, pp. 5–11, Aug. 2004.
- [14] J. L. Kelsey *et al.*, "An epidemiologic study of lifting and twisting on the job and risk for acute prolapsed lumbar intervertebral disc," *J. Orthopaedic Res.*, vol. 2, no. 1, pp. 61–66, 1984, doi: 10.1002/jor.1100020110.
- [15] W. S. Marras, S. A. Ferguson, D. Burr, K. G. Davis, and P. Gupta, "Spine loading in patients with low back pain during asymmetric lifting exertions," *Spine J.*, vol. 4, no. 1, pp. 64–75, Jan. 2004, doi: 10.1016/S1529-9430(03)00424-8.
- [16] S. Ferguson, W. Marras, and T. Waters, "Quantification of back motion during asymmetric lifting," *Ergonomics*, vol. 35, pp. 845–859, Jul. 1992, doi: 10.1080/00140139208967366.
- [17] W. Marras and K. Davis, "Spine loading during asymmetric lifting using one versus two hands," *Ergonomics*, vol. 41, pp. 817–834, Jul. 1998, doi: 10.1080/001401398186667.
- [18] H. Schmidt, A. Kettler, F. Heuer, U. Simon, L. Claes, and H.-J. Wilke, "Intradiscal pressure, shear strain, and fiber strain in the intervertebral disc under combined loading," *Spine*, vol. 32, no. 7, pp. 748–755, Apr. 2007, doi: 10.1097/01.brs.0000259059.90430.c2.
- [19] H.-K. Kim and Y. Zhang, "Estimation of lumbar spinal loading and trunk muscle forces during asymmetric lifting tasks: Application of wholebody musculoskeletal modelling in opensim," *Ergonomics*, vol. 60, no. 4, pp. 563–576, Apr. 2017, doi: 10.1080/00140139.2016.1191679.
- [20] D. D. Molinaro, A. S. King, and A. J. Young, "Biomechanical analysis of common solid waste collection throwing techniques using opensim and an EMG-assisted solver," *J. Biomech.*, vol. 104, May 2020, Art. no. 109704, doi: 10.1016/j.jbiomech.2020.109704.

- [21] S.-P. Wu, "Psychophysically determined symmetric and asymmetric lifting capacity of chinese males for one hour's work shifts," *Int. J. Ind. Ergon.*, vol. 25, no. 6, pp. 675–682, Jul. 2000, doi: 10.1016/S0169-8141(99)00055-4.
- [22] M. P. de Looze, T. Bosch, F. Krause, K. S. Stadler, and L. W. O'Sullivan, "Exoskeletons for industrial application and their potential effects on physical work load," *Ergonomics*, vol. 59, no. 5, pp. 671–681, May 2016, doi: 10.1080/00140139.2015.1081988.
- [23] A. T. Asbeck, R. J. Dyer, A. F. Larusson, and C. J. Walsh, "Biologically-inspired soft exosuit," in *Proc. IEEE 13th Int. Conf. Rehabil. Robot.*, Jun. 2013, pp. 1–8, doi: 10.1109/ICORR.2013.6650455.
- [24] P. Dolan and M. A. Adams, "The relationship between EMG activity and extensor moment generation in the erector spinae muscles during bending and lifting activities," *J. Biomech.*, vol. 26, no. 4/5, pp. 513–522, May 1993, doi: 10.1016/0021-9290(93)90013-5.
- [25] M. Abdoli-E, M. J. Agnew, and J. M. Stevenson, "An on-body personal lift augmentation device (PLAD) reduces EMG amplitude of erector spinae during lifting tasks," *Clin. Biomech.*, vol. 21, no. 5, pp. 456–465, Jun. 2006, doi: 10.1016/j.clinbiomech.2005.12.021.
- [26] E. P. Lamers, A. J. Yang, and K. E. Zelik, "Feasibility of a biomechanically-assistive garment to reduce low back loading during leaning and lifting," *IEEE Trans. Biomed. Eng.*, vol. 65, no. 8, pp. 1674–1680, Aug. 2018, doi: 10.1109/TBME.2017.2761455.
- [27] M. M. Alemi, J. Geissinger, A. A. Simon, S. E. Chang, and A. T. Asbeck, "A passive exoskeleton reduces peak and mean EMG during symmetric and asymmetric lifting," *J. Electromyography Kinesiology*, vol. 47, pp. 25–34, Aug. 2019, doi: 10.1016/j.jelekin.2019.05.003.
- [28] A. S. Koopman, I. Kingma, M. P. de Looze, and J. H. van Dieën, "Effects of a passive back exoskeleton on the mechanical loading of the low-back during symmetric lifting," *J. Biomech.*, vol. 102, Mar. 2020, Art. no. 109486, doi: 10.1016/j.jbiomech.2019.109486.
- [29] S. Toxiri et al., "Back-support exoskeletons for occupational use: An overview of technological advances and trends," IISE Trans. Occupational Ergonom. Human Factors, vol. 7, no. 3/4, pp. 237–249, Oct. 2019, doi: 10.1080/24725838.2019.1626303.
- [30] M. Abdoli-E and J. M. Stevenson, "The effect of on-body lift assistive device on the lumbar 3D dynamic moments and EMG during asymmetric freestyle lifting," *Clin. Biomech.*, vol. 23, no. 3, pp. 372–380, Mar. 2008, doi: 10.1016/j.clinbiomech.2007.10.012.
- [31] P. Dolan, M. Earley, and M. A. Adams, "Bending and compressive stresses acting on the lumbar spine during lifting activities," *J. Biomech.*, vol. 27, no. 10, pp. 1237–1248, Oct. 1994, doi: 10.1016/0021-9290(94)90277-1.
- [32] S. Toxiri et al., "Rationale, implementation and evaluation of assistive strategies for an active back-support exoskeleton," Frontiers Robot. AI, vol. 5, pp. 1–14, 2018, doi: 10.3389/frobt.2018.00053.
- [33] B. Chen, L. Grazi, F. Lanotte, N. Vitiello, and S. Crea, "A real-time lift detection strategy for a hip exoskeleton," *Frontiers Neurorobotics*, vol. 12, pp. 1–11, 2018, doi: 10.3389/fnbot.2018.00017.
- [34] T. Zhang and H. Huang, "A lower-back robotic exoskeleton: Industrial handling augmentation used to provide spinal support," *IEEE Robot. Autom. Mag.*, vol. 25, no. 2, pp. 95–106, Jun. 2018, doi: 10.1109/MRA.2018.2815083.
- [35] X. Yong, Z. Yan, C. Wang, C. Wang, N. Li, and X. Wu, "Ergonomic mechanical design and assessment of a waist assist exoskeleton for reducing lumbar loads during lifting task," *Micromachines*, vol. 10, no. 7, pp. 1–18, Jul. 2019, doi: 10.3390/mi10070463.
- [36] U. Heo, S. J. Kim, and J. Kim, "Backdrivable and fully-portable pneumatic back support exoskeleton for lifting assistance," *IEEE Robot. Autom. Lett.*, vol. 5, no. 2, pp. 2047–2053, Apr. 2020, doi: 10.1109/LRA.2020.2969169.
- [37] M. Cempini, S. M. M. De Rossi, T. Lenzi, N. Vitiello, and M. C. Carrozza, "Self-alignment mechanisms for assistive wearable robots: A kinetostatic compatibility method," *IEEE Trans. Robot.*, vol. 29, no. 1, pp. 236–250, Feb. 2013, doi: 10.1109/TRO.2012.2226381.
- [38] R. Norman, R. Wells, P. Neumann, J. Frank, H. Shannon, and M. Kerr, "A comparison of peak vs cumulative physical work exposure risk factors for the reporting of low back pain in the automotive industry," *Clin. Biomech.*, vol. 13, no. 8, pp. 561–573, Dec. 1998, doi: 10.1016/S0268-0033(98)00020-5.
- [39] B. Chen, F. Lanotte, L. Grazi, N. Vitiello, and S. Crea, "Classification of lifting techniques for application of a robotic hip exoskeleton," *Sensors*, vol. 19, no. 4, Jan. 2019, Art. no. 4, doi: 10.3390/s19040963.
- [40] S. Grosu et al., "Driving robotic exoskeletons using cable-based transmissions: A qualitative analysis and overview," Appl. Mech. Rev., vol. 70, no. 6, Nov. 2018, Art. no. 060801, doi: 10.1115/1.4042399.

- [41] A. T. Asbeck, S. M. M. De Rossi, I. Galiana, Y. Ding, and C. J. Walsh, "Stronger, smarter, softer: Next-generation wearable robots," *IEEE Robot. Autom. Mag.*, vol. 21, no. 4, pp. 22–33, Dec. 2014, doi: 10.1109/MRA.2014.2360283.
- [42] Y. Mao and S. K. Agrawal, "Design of a cable-driven arm exoskeleton (CAREX) for neural rehabilitation," *IEEE Trans. Robot.*, vol. 28, no. 4, pp. 922–931, Aug. 2012, doi: 10.1109/TRO.2012.2189496.
- [43] F. A. Panizzolo *et al.*, "A biologically-inspired multi-joint soft exosuit that can reduce the energy cost of loaded walking," *J. NeuroEng. Rehabil.*, vol. 13, May 2016, Art. no. 43, doi: 10.1186/s12984-016-0150-9.
- [44] H. K. Ko, S. W. Lee, D. H. Koo, I. Lee, and D. J. Hyun, "Waist-assistive exoskeleton powered by a singular actuation mechanism for prevention of back-injury," *Robot. Auton. Syst.*, vol. 107, pp. 1–9, Sep. 2018, doi: 10.1016/j.robot.2018.05.008.
- [45] X. Yang et al., "Spine-inspired continuum soft exoskeleton for stoop lifting assistance," *IEEE Robot. Autom. Lett.*, vol. 4, no. 4, pp. 4547–4554, Oct. 2019, doi: 10.1109/LRA.2019.2935351.
- [46] S. Lee, S. Crea, P. Malcolm, I. Galiana, A. Asbeck, and C. Walsh, "Controlling negative and positive power at the ankle with a soft exosuit," in *Porc. IEEE Int. Conf. Robot. Automat.*, May 2016, pp. 3509–3515, doi: 10.1109/ICRA.2016.7487531.
- [47] K. A. Witte, A. M. Fatschel, and S. H. Collins, "Design of a lightweight, tethered, torque-controlled knee exoskeleton," in *Proc. Int. Conf. Rehabil. Robot.*, Jul. 2017, pp. 1646–1653, doi: 10.1109/ICORR.2017.8009484.
- [48] S. Toxiri, J. Ortiz, J. Masood, J. Fernández, L. A. Mateos, and D. G. Caldwell, "A wearable device for reducing spinal loads during lifting tasks: Biomechanics and design concepts," in *Proc. IEEE Int. Conf. Robot. Biomimetics*, Dec. 2015, pp. 2295–2300, doi: 10.1109/RO-BIO.2015.7419116.
- [49] M. Abdoli-Eramaki, J. M. Stevenson, S. A. Reid, and T. J. Bryant, "Mathematical and empirical proof of principle for an on-body personal lift augmentation device (PLAD)," *J. Biomech.*, vol. 40, no. 8, pp. 1694–1700, Jan. 2007, doi: 10.1016/j.jbiomech.2006.09.006.
- [50] J. H. van Dieën, P. van der Burg, T. A. Raaijmakers, and H. M. Toussaint, "Effects of repetitive lifting on kinematics: Inadequate anticipatory control or adaptive changes?," *J. Motor Behav.*, vol. 30, no. 1, pp. 20–32, Mar. 1998, doi: 10.1080/00222899809601319.
- [51] U. Lee, C.-W. Pan, and E. Rouse, "Empirical characterization of a high-performance exterior-rotor type brushless DC motor and drive," in *Proc. IEEE/RSJ Int. Conf. Intell. Robots Syst.*, Nov. 2019, pp. 8018–8025, doi: 10.1109/IROS40897.2019.8967626.
- [52] A. Mazumdar et al., "Synthetic fiber capstan drives for highly efficient, torque controlled, robotic applications," *IEEE Robot. Autom. Lett.*, vol. 2, no. 2, pp. 554–561, Apr. 2017, doi: 10.1109/LRA.2016.2646259.
- [53] M. B. Yandell, D. M. Ziemnicki, K. A. McDonald, and K. E. Zelik, "Characterizing the comfort limits of forces applied to the shoulders, thigh and shank to inform exosuit design," *PLOS ONE*, vol. 15, no. 2, Feb. 2020, Art. no. e0228536, doi: 10.1371/journal.pone.0228536.
- [54] C. D. Fryar, D. Kruszon-Moran, Q. Gu, and C. L. Ogden, "Mean body weight, height, waist circumference, and body mass index among adults: United States, 1999-2000 through 2015-2016," *Nat. Health Statist. Rep.*, vol. 122, no. 122, pp. 1–16, 2018.
- [55] S. L. Delp et al., "OpenSim: Open-source software to create and analyze dynamic simulations of movement," *IEEE Trans. Biomed. Eng.*, vol. 54, no. 11, pp. 1940–1950, Nov. 2007, doi: 10.1109/TBME.2007.901024.
- [56] A. Seth et al., "OpenSim: Simulating musculoskeletal dynamics and neuromuscular control to study human and animal movement," PLOS Comput. Biol., vol. 14, no. 7, Jul. 2018, Art. no. e1006223, doi: 10.1371/journal.pcbi.1006223.
- [57] E. Beaucage-Gauvreau et al., "Validation of an opensim full-body model with detailed lumbar spine for estimating lower lumbar spine loads during symmetric and asymmetric lifting tasks," Comput. Methods Biomech. Biomed. Eng., vol. 22, no. 5, pp. 451–464, Apr. 2019, doi: 10.1080/10255842.2018.1564819.
- [58] D. Stegeman and H. Hermens, "Standards for suface electromyography: The European project surface EMG for non-invasive assessment of muscles (SENIAM)," Proc. 3rd General SENIAM Workshop Surface Electromyography, vol. 1, pp. 108–112, Jan. 2007.
- [59] P. Konrad, "ABC of EMG A Practical Introduction to Kinesiological Electromyography," Noraxon USA Inc., vol. 1.4, pp. 29, Mar. 2006.
- [60] M. A. Sherman, A. Seth, and S. L. Delp, "What is a moment arm? Calculating muscle effectiveness in biomechanical models using generalized coordinates," in *Proc. ASME Des. Eng. Tech. Conf. ASME Des. Eng. Tech. Conf.*, vol. 2013, pp. 1–18, Aug. 2013, doi: 10.1115/DETC2013-13633.

- [61] M. Christophy, N. A. Faruk Senan, J. C. Lotz, and O. M. O'Reilly, "A musculoskeletal model for the lumbar spine," *Biomech. Model. Mechanobiology*, vol. 11, no. 1, pp. 19–34, Jan. 2012, doi: 10.1007/s10237-011-0290-6.
- [62] M. P. de Looze, H. M. Toussaint, J. H. van Dieën, and H. C. G. Kemper, "Joint moments and muscle activity in the lower extremities and lower back in lifting and lowering tasks," *J. Biomech.*, vol. 26, no. 9, pp. 1067–1076, Sep. 1993, doi: 10.1016/S0021-9290(05)80006-5.
- [63] K. G. Davis, W. S. Marras, and T. R. Waters, "Evaluation of spinal loading during lowering and lifting," *Clin. Biomech.*, vol. 13, no. 3, pp. 141–152, Apr. 1998, doi: 10.1016/S0268-0033(97)00037-5.



Jared M. Li received the B.S. and M.S. degrees in mechanical engineering from the Georgia Institute of Technology, Atlanta, GA, USA, in 2019 and 2020, respectively.

He is currently a Wearable Robotics Research Associate with the Florida Institute for Human and Machine Cognition, Pensacola, Florida, where his work centers around the design and control of a lower-body exoskeleton for load-carriage. His research interests include bioinspired design of soft exosuits, intent recognition control of wearable robotics, and biome-

chanical analysis of human motion.



Dean D. Molinaro (Student Member, IEEE) received the B.S. degree in mechanical engineering from the University of Florida, Gainesville, FL, USA, in 2017. He is currently working toward the Ph.D. degree in robotics from the Georgia Institute of Technology, Atlanta, GA, USA.

His research interests include the integration of wearable robotic control, artificial intelligence, and human biomechanics.



Andrew S. King received the B.S. degree in mechanical engineering in 2021 from the Georgia Institute of Technology, Atlanta, GA, USA, where he is currently working toward the M.S. degree in mechanical engineering.

He is currently an Associate Mechanical Engineer with iRobot Corporation, Bedford, MA, USA, where his work focuses on the development of new robotic home cleaning devices. His research interests include the practical application of robotics to everyday life, including consumer robots, and wearable exosuits.



Anirban Mazumdar (Member, IEEE) received the S.B., S.M., and Ph.D. degrees in mechanical engineering from the Massachusetts Institute of Technology, Cambridge, MA, USA, in 2007, 2009, and 2013, respectively.

He completed his Postdoctoral Research with the Robotics Research and Development Group, Sandia National Laboratories, Albuquerque, NM, USA. He is currently an Assistant Professor with the Woodruff School of Mechanical Engineering, Georgia Institute of Technology, Atlanta, GA, USA. His research

interests include wearable systems, mobile robots, and automation for high consequence systems.



Aaron J. Young received the B.S. degree in biomedical engineering from Purdue University, West Lafayette, IN, USA, in 2009, and the M.S. and Ph.D. degrees in biomedical engineering from Northwestern University, Evanston, IL, USA, in 2011 and 2014, respectively.

He is currently an Assistant Professor with the Woodruff School of Mechanical Engineering, the Georgia Institute of Technology, Atlanta, GA, USA, and has directed the Exoskeleton and Prosthetic Intelligent Controls Lab since 2016. His research interests

include advanced control systems for robotic prosthetic and exoskeleton systems for improving lower limb human mobility.